Molecular Blending by Polymerization of Intercalated Solvent. Poly(γ-benzyl-L-glutamate)/Benzyl Methacrylate as a Model System

C. S. J. van Hooy-Corstjens† and S. Rastogi*,‡

Faculty of Medicine, University of Maastricht, P.O. Box 616, 6200MD Maastricht, and Department of Chemical Engineering, Dutch Polymer Institute/Eindhoven University of Technology, P.O. Box 513, 5600 MB Eindhoven, The Netherlands

Received October 27, 2005; Revised Manuscript Received February 5, 2006

The aim of the present research is to obtain blending between a polymer and a (polymerized) solvent on the molecular level. Because of its rigid rod structure, poly(γ-benzyl-L-glutamate) (PBLG) is chosen as the polymer. Benzyl methacrylate (BzMA) has been chosen as the solvent for two reasons. First, the structure of the solvent is very similar to the structure of the side chain of PBLG, favoring interactions between the two materials. Second, the solvent can be polymerized, because of the presence of a C═C bond. In cast films of PBLG and BzMA separate zones of the polymer and solvent are present. Wide-angle X-ray diffraction and Raman results show that upon heating the cast films homogenization occurs and solvent molecules intercalate between the helices of PBLG. At 150 °C a hexagonal packing is obtained. The dimensions of the obtained packing depend on the solvent concentration, which confirms that solvent molecules are indeed present within the crystalline lattice. DSC experiments imply that the observed changes upon heating correspond to thermodynamic processes. On cooling the homogeneous samples, disordering of the hexagonal packing occurs. Polymerization of the homogeneous samples results in a disordering of the hexagonal packing and in a contraction of the unit cell. The latter once more confirms that solvent molecules are indeed present within the crystalline lattice. The applied principle of polymerization of a solvent in a molecular homogeneous system can be favorable for many applications, for which morphology control at the molecular level is required.

1. Introduction

Continuously improving technologies result in more and more sophisticated demands for polymer systems. Due to miniaturization of, e.g., electronic devices, morphology control on the nanometer scale is already required. A possible route to obtain blending at such a level is to start from a polymer and a monomer. Once a homogeneous state is obtained, the monomer can be converted into a polymer, e.g., by means of UV irradiation. In an attempt to obtain blending via this route, use is made of a model system consisting of poly(γ-benzyl-L-glutamate) (PBLG) and benzyl methacrylate (BzMA). Moreover, there exists a range of polymer−solvent complexes where the polymer structure is stabilized by the presence of a solvent; for example, in spider silk the presence of a solvent with a salt prior to spinning inhibits crystallization of peptides.

PBLG, first synthesized in the 1930s, is a synthetic polypeptide with the side group $-(CH_2)_2(C{=}O)OCH_2C_6H_5$. This polypeptide, which is soluble in several organic solvents, is regarded as an ideal model of a liquid crystalline polymer. In solution, hydrogen bonds can be formed between the oxygen of a carbonyl group and the hydrogen of an amide group, four groups further down the main chain, resulting in an 18/5 α-helical structure.[1] Since the hydrogen bonds prevent chain flexibility, the molecules behave as rather rigid rods. These rods are only stable in solvents which do not interfere with the hydrogen bonds, so-called helicoidal solvents. Molecular aggregation of PBLG in such solvents has been studied by various methods.[2−9] The phase diagram of these PBLG solutions is in agreement with the typical phase diagram of rodlike molecules as proposed by Flory in 1956.[10,11] At low polymer concentrations the solution is isotropic, whereas at high concentrations a liquid crystalline solution is obtained. Between these two single-phase regions there is a biphasic region in which both phases can coexist.[11,12]

Some PBLG solutions form a self-supporting gel. These gels, especially the ones formed in benzyl alcohol, have been studied by many researchers.[13−19] Different explanations have been given for the gelation process. Most likely, gel formation results from L−L phase separation combined with crystallization. The crystalline junctions can comprise either polymer crystals or solvent-included complex phases.[14,15]

In this paper the behavior of PBLG in the presence of BzMA will be described.[20] BzMA is chosen as the solvent for two different reasons. First of all, the structure of this solvent is very similar to the structure of the side chain of PBLG. This can be favorable to obtain intercalation of the solvent between the PBLG helices, resulting in the formation of a complex phase. Moreover, the solvent contains a C═C bond, which gives the possibility to polymerize the solvent.

To form a basis for understanding the results of PBLG/BzMA systems, first the results upon casting pure PBLG from dichloromethane will be described. The behavior of PBLG/BzMA films has been studied by wide-angle X-ray diffraction, differential scanning calorimetry, and Raman spectroscopy. At the end of the paper the polymerization of BzMA in the PBLG/BzMA samples will be discussed.

* To whom correspondence should be addressed. E-mail: s.rastogi@tue.nl.
† University of Maastricht.
‡ Dutch Polymer Institute/Eindhoven University of Technology.

10.1021/bm050817q CCC: $33.50
Published on Web 04/20/2006

2. Experimental Section

2.1. Materials and Sample Preparation. Poly(γ-benzyl-L-glutamate) with a molar mass of approximately 220 kg·mol^{-1} and a polydispersity of 1.12 was obtained from Sigma Chemical Laboratory. Benzyl methacrylate with a purity of 96% and dichloromethane (purity >99%) were purchased from Aldrich Chemical Co. and used without purification. Aldrich also supplied the inhibitor benzoquinone and the UV initiator 2,2-dimethoxy-2-phenylacetophenone (DMPA), which has an absorption maximum at 342 nm.

Samples were prepared by dissolving PBLG and BzMA (containing either inhibitor or 2 wt % UV initiator) in dichloromethane. The solutions were poured into a Petri dish and dried in air. The films thus obtained, in which the concentration of PBLG varied between 20 and 100 wt %, were sealed into Lindemann capillaries or stainless steel pans.

2.2. Techniques. To perform in situ heating experiments with wide-angle X-ray diffraction (WAXS) or Raman spectroscopy, the sealed capillaries were placed in a holder which was fixed on a Linkam THMS 600 hot stage. The hot stage was controlled with a TMS-92 controller and a Linkam LN2 cooling unit. The applied heating and cooling rates were 5 or 10 °C·min^{-1}. To polymerize the solvent, the samples were irradiated for about 30 min with a Philips PL-S 9W/10 UV lamp, having a wavelength of 365 nm.

Time-resolved WAXS experiments were performed at beamline ID11 of the European Synchrotron Radiation Facility (ESRF) in Grenoble, France. The wavelength was set at 1 Å (E = 12.4 keV) for most experiments. Only during polymerization of pure BzMA (Figure 5) a wavelength of 0.76 Å was applied. X-ray patterns were recorded with a CCD detector, and the exposure time during recording of a spectrum was approximately 20 s.

A Dilor Labram system, coupled with an air-cooled CCD array detector, was used to record the Raman spectra, which were obtained in the backscattering mode. The 532 nm line of a Spectra-Physics Nd:YVO_4 laser was used as the incident beam.

Dynamic scanning calorimetry (DSC) measurements were performed with a Perkin-Elmer DSC-7. A small piece of a film was weighed in a stainless steel pan, and the pan was closed with a stainless steel cover containing a rubber O-ring. The pans contained between 15 and 30 mg of material. To measure phase transitions, the samples were heated to 150 °C at a rate of 5 °C·min^{-1}.

3. Results and Discussion

3.1. Pure PBLG. Before the PBLG/BzMA systems are discussed, Raman data and wide-angle X-ray diffraction results of pure PBLG will be described. Raman experiments were performed to check whether casting from dichloromethane results in a random coil or in an α-helical conformation. Differences in the backbone vibrations are used to distinguish between these conformational situations.[21]

In Figure 1 the Raman spectra of a cast film of PBLG and a sample which has been heated to 150 °C are depicted. The C═O stretching band (amide I mode) of the cast film is observed at 1654 cm^{-1}, whereas the C−C−N symmetric stretching band appears at 929 cm^{-1}. These values are in close accordance with the values of the α-helical conformation of PBLG, for which the bands have been reported at 1652 and 934 cm^{-1}, respectively.[22] In the case of a random coil, the reflection for the amide I band would be shifted to a slightly lower frequency and the reflection of the C−C−N symmetric stretching vibration band about 10 cm^{-1} to higher frequency. The slight deviations between our measured and the literature values is in the opposite frequency direction; hence, it can be concluded that in the cast film the PBLG molecules adopt an α-helical conformation.

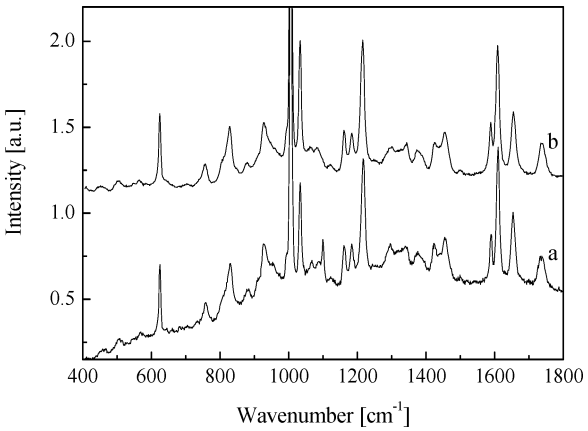

Figure 1. Raman spectra of pure PBLG: (a) cast film at room temperature, (b) sample after heating to 150 °C.

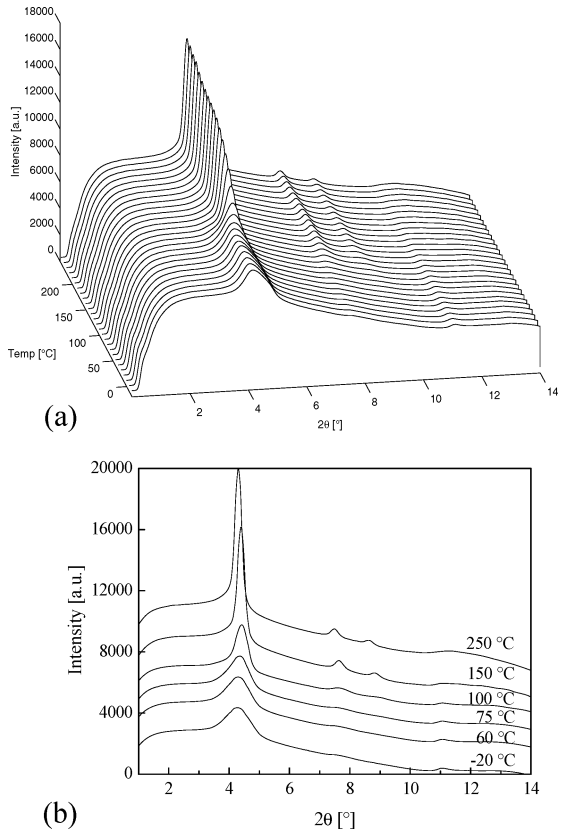

Figure 2. WAXS patterns (λ = 1 Å) upon heating a cast film of pure PBLG: (a) 3-D representation, (b) 2-D representation.

Upon heating the sample to 150 °C, no shift in the Raman bands is observed, indicating that the α-helical conformation is maintained.

Figure 2 represents 3-D and 2-D plots of WAXS patterns of a film of PBLG, cast from dichloromethane. The cast film shows a broad, asymmetric reflection around $2\theta = 4.2°$ (d = 13.7 Å). The diffraction pattern is weak, and no clear crystal modification can be assigned. Upon heating the sample to 150 °C, the reflection sharpens and shifts to $2\theta = 4.4°$ (d = 13 Å). Furthermore, with gradually increasing temperature two new reflections are observed at $2\theta = 7.6°$ (d = 7.5 Å) and $2\theta = 8.9°$ (d = 6.5 Å). The ratio between the d values is close to $1:(1/\sqrt{3}):(1/2)$. This suggests that the chains pack in a hexagonal phase and the observed reflections correspond to the (100), (110), and (200) planes, respectively. Also in literature, for

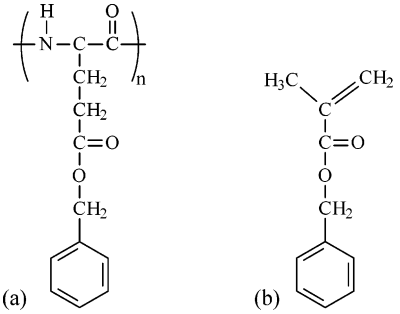

Figure 3. Structural formulas of (a) PBLG and (b) BzMA.

PBLG several phases containing a hexagonal packing have been described. [23,24]

3.2. Phase Behavior of PBLG/BzMA Systems. The behavior of cast films of PBLG and BzMA has been studied by WAXS, Raman spectroscopy, and differential scanning calorimetry (DSC). Compared to solvents used so far in PBLG/solvent studies, BzMA is quite unique since the structure of the solvent is nearly similar to that of the side chain of PBLG (see Figure 3). Moreover, the presence of a C═C bond gives a possibility to polymerize the solvent.

3.2.1. Formation of Polymer−Solvent Complexes on Heating: WAXS Results. Samples with different concentrations of PBLG have been measured, for which the WAXS data show some differences. As an illustration, the WAXS data of samples with a relatively high (60 wt %) and a relatively low (20 wt %) polymer content will be discussed.[25]

PBLG/BzMA (60/40 wt %). Figure 4a gives a 3-D representation of the integrated WAXS data upon heating a 60/40 wt % PBLG/BzMA sample, while in Figure 4b curves at some characteristic temperatures are depicted.

In the starting material, a relatively high, diffuse intensity is observed in the small-angle region ($2\theta = 0-1°$), close to the beamstop. An explanation for the presence of this high intensity could be that in the cast samples separation between polymer-rich and solvent-rich domains exists. Due to electron density differences between PBLG and BzMA, the presence of separate zones results in a high intensity in the small-angle region, close to the beamstop. Besides the high intensity in the small-angle region, the X-ray diffraction pattern shows three relatively broad reflections and one weak but sharp reflection at higher angles. The first broad reflection, which is partially overlapping with the relatively high intensity close to the beamstop is positioned at $2\theta = 1.7°$ ($d = 34$ Å), while the other reflections are observed at $2\theta = 3.5°$ ($d = 16.4$ Å), $2\theta = 11.6°$ ($d = 4.9$ Å, relatively sharp), and $2\theta = 13°$ ($d = 4.4$ Å), respectively.

Upon heating the sample, the intensity in the small-angle region and the reflection at $2\theta = 1.7°$ ($d = 34.0$ Å) disappear. This suggests homogenization of the system on heating. To gain more insight into the changes which occur upon homogenization, the integrated diffraction patterns in the range of $2\theta = 0-3°$ are shown in Figure 4b. The intensity in the small-angle region starts to drop around 80 °C, while the reflection at $2\theta = 1.7°$ ($d = 34.0$ Å) disappears at approximately 130 °C.

The disappearance of the intensity in the small-angle region implies that homogenization between the polymer-rich and solvent-rich domains occurs on heating. The fact that the reflection at $2\theta = 1.7°$ ($d = 34.0$ Å) also disappears during the homogenization process suggests that two different types of domains are present in the cast films. A detailed explanation for this behavior requires further experimentation, and this will be discussed later in this paper.

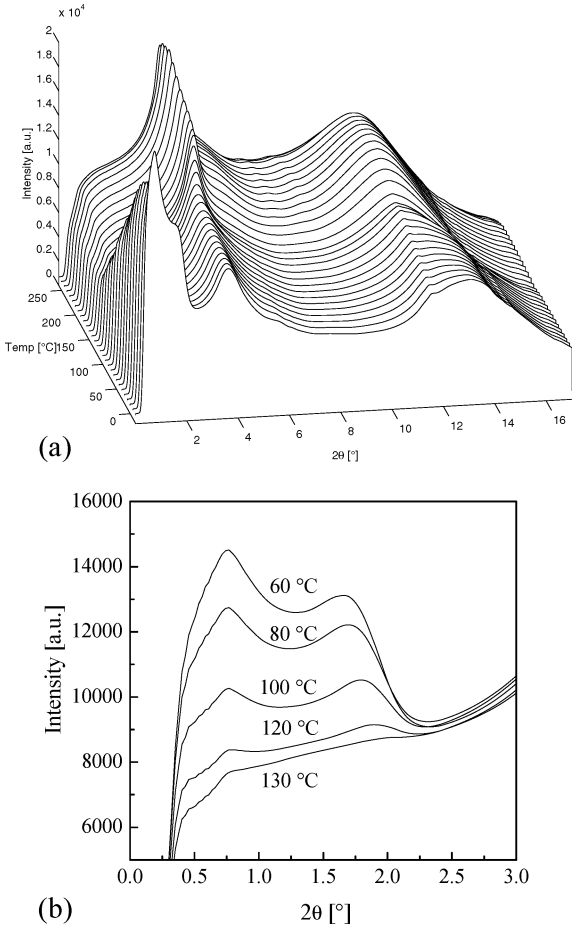

Figure 4. WAXS patterns ($\lambda = 1$ Å) upon heating a 60/40 wt % PBLG/BzMA sample: (a) 3-D representation, (b) 2-D representation close to the beamstop.

Simultaneously with the homogenization, the reflection at $2\theta = 11.6°$ ($d = 4.9$ Å) disappears, while the reflection at large diffraction angle ($2\theta = 13°$, $d = 4.4$ Å) shifts to a slightly lower value. At 200 °C this reflection is positioned at $2\theta = 11.2°$ ($d = 5.1$ Å). At this temperature a relatively sharp reflection is also present at $2\theta = 4.1°$ ($d = 14$ Å). This reflection shows overlapping with a broad reflection at a slightly larger diffraction angle. The position of the sharp reflection ($2\theta = 4.1°$, $d = 14.0$ Å) is very close to that of the most intense reflection present in the diffraction pattern of pure PBLG ($2\theta = 4.4°$ ($d = 13$ Å)) (Figure 2). This suggests that, similar to pure PBLG, also for the 60/40 wt % PBLG/BzMA sample a hexagonal unit cell is obtained. The small increase in the d value of the (100) reflection of the hexagonal phase indicates that the crystalline lattice is influenced by the solvent. This is confirmed by the fact that above 150 °C also a relatively broad reflection ($2\theta \approx 4.7°$ ($d \approx 12.2$ Å)), which is overlapping with the (100) reflection, is observed. This relatively broad reflection is not observed for pure PBLG, and therefore, this reflection should be arising from the presence of the solvent.

To be able to draw a conclusion about the origin of this reflection, the WAXS patterns of unpolymerized and polymerized BzMA (PBzMA) are depicted in Figure 5. In the unpolymerized sample only one reflection is observed. This reflection, with a d spacing of about 4.8 Å, corresponds to the interaction between phenyl rings. Upon polymerization, another reflection is observed around 11.8 Å ($2\theta \approx 3.7°$), corresponding to the interchain distance in PBzMA.

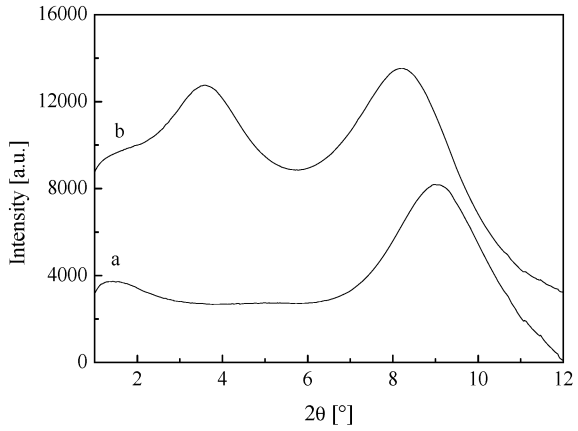

Figure 5. WAXS patterns ($\lambda = 0.76$ Å) of a BzMA sample: (a) unpolymerized and (b) polymerized samples.

A possible explanation for the broad reflection in the PBLG/BzMA system at 12.2 Å ($2\theta \approx 4.7°$) can be that the BzMA is polymerized, giving rise to the broad reflection around 12.2 Å ($2\theta \approx 4.7°$). However, as will be shown later in this paper, the presence of a peak at 1636 cm^{-1} (C═C stretching vibration, Figure 10) in the Raman spectrum indicates that at this temperature (150 °C) BzMA is not polymerized yet. It is therefore suggested that the broad reflection is arising from intercalation of the solvent molecules within the crystalline lattice. The similarity in the structure of BzMA and the side chain of PBLG makes it likely that some polymer chains in the hexagonal unit cell can be replaced by solvent molecules. In this way channels in which the solvent molecules can be placed are obtained. Phenyl−phenyl interaction between the polymer and the solvent results in a regular ordering of the solvent molecules, thus leading to the observed reflection, similar to that of PBzMA. Hence, though the solvent is not polymerized yet, the regular ordering of the molecules within the crystalline lattice gives rise to a reflection which is in agreement with the interchain distance in PBzMA.

To gain further insight into the origin of the WAXS patterns (high intensity in the small-angle region and reflections indicating a hexagonal packing), experimental observations at low polymer concentration will be presented.

PBLG/BzMA (20/80 wt %). The WAXS data upon heating a 20/80 wt % PBLG/BzMA sample are depicted in Figure 6. In this figure, (a) gives a 3-D representation of the integrated patterns, (b) depicts the X-ray diffraction patterns at small diffraction angles ($2\theta = 0-3°$), and (c) gives the data at larger diffraction angles ($2\theta = 2-17°$).

In the cast film, a high intensity in the small-angle region, close to the beamstop, is observed. Similar to the 60 wt % PBLG sample, this is attributed to electron density differences between polymer-rich and solvent-rich domains, which are present in the cast films. The difference from the 60 wt % PBLG sample is that, for a similar sample thickness, for the 20 wt % PBLG sample the intensity at the beamstop is increased and the position of the maximum is shifted to lower diffraction angles. The latter implies that, due to the presence of more solvent, larger domains are formed. It seems logical that, for low polymer concentration, relatively less polymer will be present in the solvent-rich domains. This results in an increased contrast between the polymer-rich and solvent-rich domains, which can explain the higher intensity near the beamstop. Besides the high intensity close to the beamstop, two very broad reflections are present around $2\theta = 3.4°$ ($d = 16.9$ Å) and $2\theta = 12.5°$ ($d = 4.6$ Å), which in terms of position have similarities with those of the

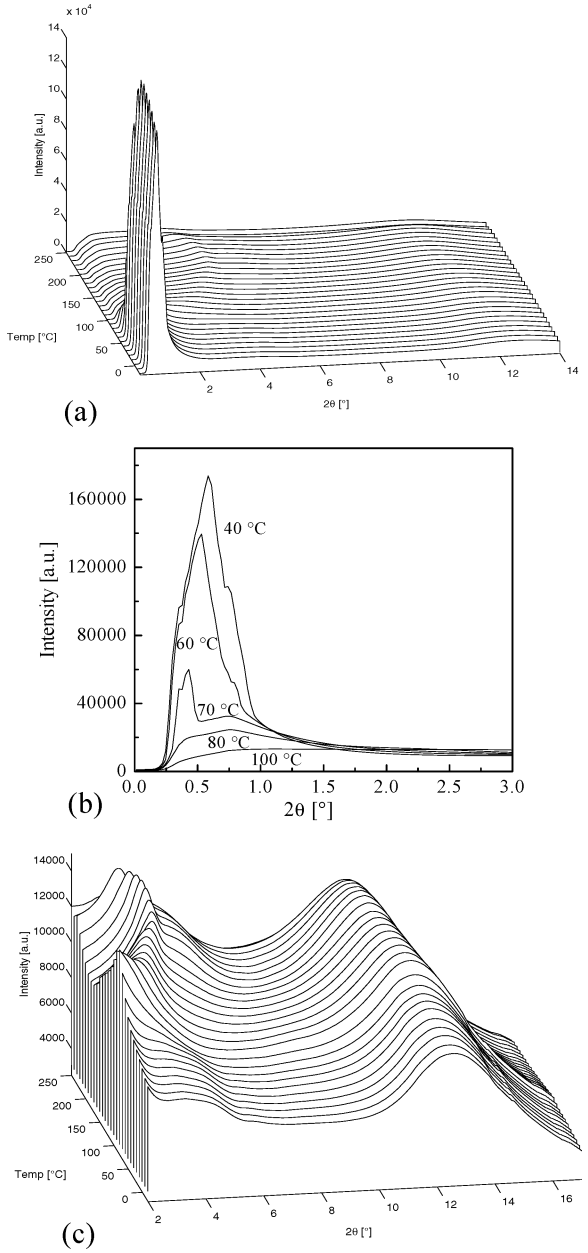

Figure 6. WAXS patterns ($\lambda = 1$ Å) upon heating a 20/80 wt % PBLG/BzMA sample: (a) 3-D representation, (b) 2-D representation close to the beamstop, (c) 3-D representation at larger diffraction angles.

60/40 wt % PBLG/BzMA sample. Upon heating, the high intensity close to the beamstop drops, and around 80 °C it completely vanishes. This suggests that at this temperature homogenization between the polymer-rich and solvent-rich domains is complete. Also the reflection at $2\theta = 3.4°$ ($d = 16.9$ Å) disappears upon heating.

After homogenization, the incoming of a relatively sharp reflection, which overlaps with a much broader reflection, is observed. The reflection, which at 200 °C is present at $2\theta = 3.9°$ ($d = 14.9$ Å), is again assigned to the presence of a hexagonal packing, while the overlapping broad reflection is attributed to a regular ordering of the solvent molecules due to intercalation between the polymer chains. Besides the observations stated above, the reflection at $2\theta = 12.5°$ ($d = 4.6$ Å) shifts to a slightly smaller diffraction angle ($2\theta = 11.2°$ ($d = 5.1$ Å)) at 200 °C.

The changes which occur after homogenization of the cast film are very similar to those of the 60 wt % PBLG sample.

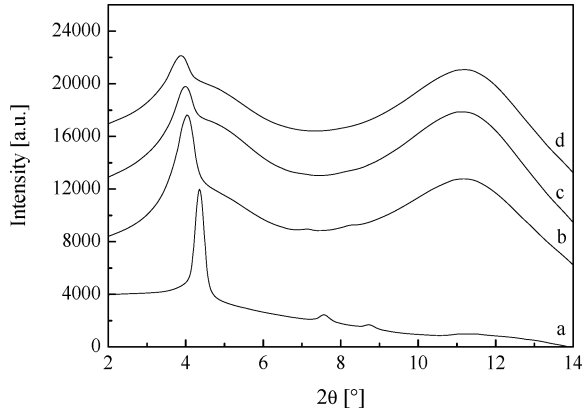

Figure 7. WAXS patterns at 200 °C for PBLG/BzMA samples: (a) pure PBLG, (b) PBLG/BzMA (60/40 wt %), (c) PBLG/BzMA (35/65 wt %), (d) PBLG/BzMA (20/80 wt %).

However, some differences in the X-ray diffraction patterns exist between samples with different polymer concentrations. To illustrate the differences, a comparison between samples with different polymer concentrations (in some cases also including 35 wt % PBLG) will be made in the next section.

Influence of the Polymer Concentration of the WAXS Results. Differences in the WAXS patterns can be summarized as follows.

(1) The intensity in the small-angle region, which is characteristic for the presence of polymer-rich and solvent-rich domains in the cast films, increases with increasing solvent concentration. This suggests that the contrast between the domains increases with solvent concentration.

(2) The presence of a reflection at $d = 34$ Å ($2\theta = 1.7°$) in the 60/40 wt % PBLG/BzMA sample suggests that, besides the separation between polymer-rich and solvent-rich domains, another type of domain formation occurs in the cast film. A regular ordering in either the polymer-rich or solvent-rich domains gives rise to the reflection at $d = 34$ Å. On the basis of the present results, it is unfortunately not possible to distinguish between the two possibilities. The reflection at $d = 34$ Å ($2\theta = 1.7°$) is not observed for the 20/80 wt % PBLG/BzMA sample, implying that this second kind of domain formation depends on the polymer concentration.

(3) The reflection present at $d = 16$ Å ($2\theta = 3.1°$) in the cast films suggests an order close to a hexagonal packing for samples with a high polymer concentration. It is anticipated that this regular ordering of the helices occurs within the polymer-rich domains. Broadening of this reflection is observed with decreasing polymer concentration, which is a result of loss in the long-range order due to the low polymer concentration.

(4) By comparing the results for homogeneous PBLG/BzMA samples with different polymer concentrations, it becomes clear that the position of the maximum of the sharp reflection slightly changes with polymer concentration. From Figure 7 it appears that at 200 °C for pure PBLG the reflection is observed at $2\theta = 4.4°$ ($d = 13$ Å), while for PBLG/BzMA (60/40 wt %) this reflection is found at $2\theta = 4.1°$ ($d = 14$ Å). Decreasing the polymer amount to 35 wt % results in a further shift of the reflection to $2\theta = 4.0°$ ($d = 14.3$ Å), and for the 20/80 wt % PBLG/BzMA sample this reflection is observed at $2\theta = 3.9°$ ($d = 14.9$ Å).

These data imply that the (100) reflection of the hexagonal unit cell shifts to larger values with increasing amount of solvent, suggesting that the packing of chains within the crystalline lattice is strongly influenced by the presence of solvent. In addition to a shift of the (100) reflection also broadening of this reflection is observed in the presence of solvent. The broadening of the reflection suggests loss in the long-range order of the crystalline lattice.

(5) The changes observed in the sharp reflection at approximately $2\theta = 4°$ ($d = 14.3$ Å) in the presence of solvent, combined with the presence of the broad reflection ($2\theta \approx 4.7°$, $d \approx 12.2$ Å), arising from a regular ordering of the solvent molecules, point to the presence of solvent molecules within the crystalline lattice. This implies that upon heating cast films of PBLG with BzMA a polymer−solvent crystalline (complex) phase is obtained. It is suggested that the structure of this complex phase is rather similar to that of the hexagonal phase of pure PBLG, but within the hexagonal structure some channels exist in which solvent molecules are present. Due to the presence of solvent molecules the dimensions of the unit cell are slightly larger than for pure PBLG. In addition, the unit cell dimensions increase with increasing amount of solvent.

3.2.2. Disordering in Polymer−Solvent Complexes on Cooling: WAXS Results. Figure 8 depicts WAXS patterns at 150 °C (homogeneous samples) and at room temperature, the latter obtained on cooling from 150 °C. The diffraction patterns at 150 °C show the reflections from the hexagonal packing clearer than those depicted in Figures 4 and 6. The difference between the two experiments is that the samples in Figure 8 were annealed at 150 °C before they were cooled to room temperature, whereas a continuous heating run was performed for Figures 4 and 6.

The presence of sharper and more pronounced reflections of the hexagonal packing indicates that annealing results in perfection of the crystalline lattice. Cooling the samples to room temperature results in broadening of the (100) reflection. Moreover, for samples with relatively high polymer content, the reflection arising from the ordered solvent molecules becomes less clear. These changes imply that the crystalline packing becomes less perfect, resulting in a less ordered state with less solvent ordering.

Some variations in the disordering of the (100) reflection on cooling are observed with polymer concentration. In the 35/65 wt % PBLG/BzMA sample no broadening of the (100) reflection is observed upon cooling to room temperature, but a splitting into two distinct reflections. These reflections are observed at $2\theta = 4°$ and 4.5° ($d = 14.3$ Å and 12.7 Å, respectively). The positions of these reflections are very close to the reflections of the complex phase observed at high temperatures and of pure PBLG. However, the high intensity close to the beamstop, which was present in the cast films, is not observed. Hence, it can be concluded that the samples stay rather homogeneous upon cooling and no clear separation into large polymer-rich and solvent-rich domains occurs.

3.2.3. Conformational Changes upon Heating and Subsequent Cooling of Cast Films. To observe changes in chain conformations during heating and cooling processes, the cast films have also been studied by Raman spectroscopy. Before these results are discussed, the Raman spectra of PBLG and BzMA will be compared in Figure 9a. Due to the similarity in structure of both materials, the spectra are nearly equal. However, a difference can be found in the C═O stretching vibration around 1720 cm^{-1}. Moreover, both spectra show a difference in the region around 1638 cm^{-1}. The peak at 1636 cm^{-1} in the spectrum of BzMA arises from the C═C stretching mode. On the other hand, PBLG shows a peak at 1651 cm^{-1}, arising from the C═O stretching mode of the backbone. The intensity of the peak at 1636 cm^{-1} in the BzMA spectrum is

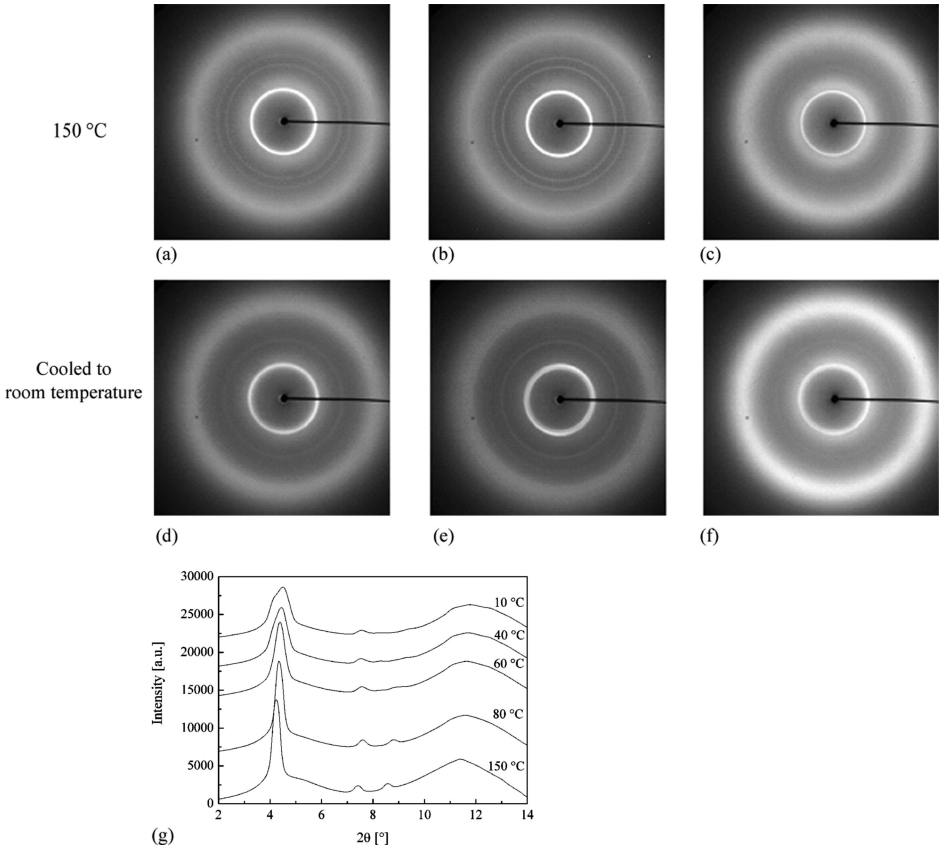

Figure 8. WAXS patterns ($\lambda = 1$ Å) upon cooling homogeneous PBLG/BzMA samples: (a, b) 60/40 wt %, (c, d) 35/65 wt %, (e, f) 20/80 wt %, at 150 °C and room temperature, respectively, (g) integrated pattern for the 35/65 wt % sample at different temperatures. The presence of reflections at 150 °C in the 2θ region 7−9°, together with reflection around 4°, corresponds to the hexagonal packing. The position of these reflections is similar to that seen for the hexagonal packing of PBLG chains in Figure 2b.

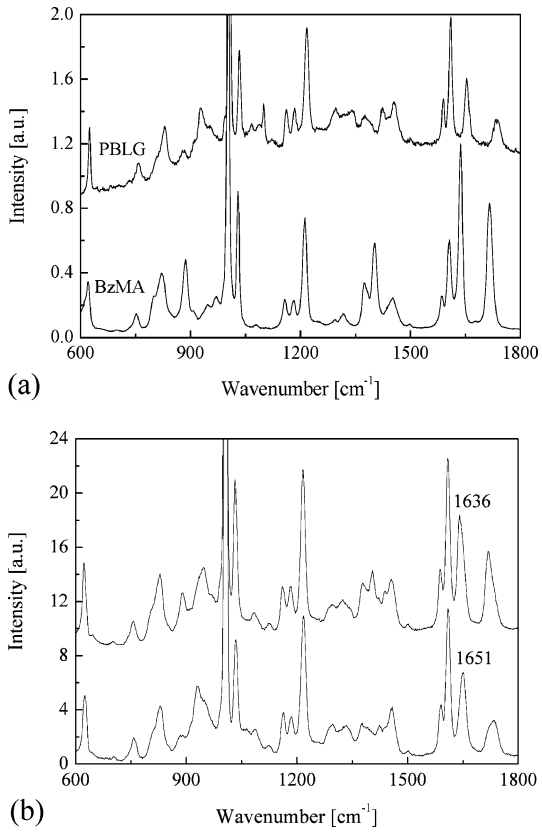

Figure 9. Raman spectra of (a) pure PBLG and BzMA and (b) 60/40 wt % PBLG/BzMA at two different positions in the sample.

much larger than that of the peak at 1651 cm^{-1} in the PBLG spectrum. To detect the peaks of both BzMA and PBLG in the PBLG/BzMA samples, it is therefore necessary to study samples with a relatively high PBLG concentration.

In Figure 9b the Raman spectra of a cast film of 60/40 wt % PBLG/BzMA are presented. The two spectra have been recorded at different positions in the sample. The presence of a peak at 929 cm^{-1} in the lower spectrum suggests the presence of α-helices of PBLG (see section 3.1). Moreover, the presence of a peak at 1651 cm^{-1} and the absence of a peak at 1636 cm^{-1} in this spectrum suggest that only PBLG is measured. The presence of peaks at 947 and 1636 cm^{-1} in the upper spectrum indicates that here only BzMA is measured. This result confirms that in the cast films polymer-rich and solvent-rich domains are present. Due to the small beam size applied in the Raman experiments (a few micrometers) situations occur in which only one of the two components present in the film is measured.

WAXS experiments indicate that the sample homogenizes upon heating. This is also clear from the lower Raman spectrum in Figure 10, which is recorded at 150 °C. This spectrum shows peaks at 1636 and 1651 cm^{-1}, indicating that both PBLG and BzMA are detected. In this spectrum the C═C stretching vibration of BzMA and the C═O stretching vibration of the backbone are measured as two separate peaks, while also the C═O stretching vibration of BzMA (1719 cm^{-1}) separates from the C═O stretching vibration of the side chain of PBLG (1733 cm^{-1}). Upon cooling the homogeneous sample to room temperature (upper spectrum Figure 10) in the region around both 1640 and 1720 cm^{-1}, the peaks of PBLG and BzMA merge together. A possible explanation can be that the presence of solvent disturbs the helical conformation of PBLG upon cooling,

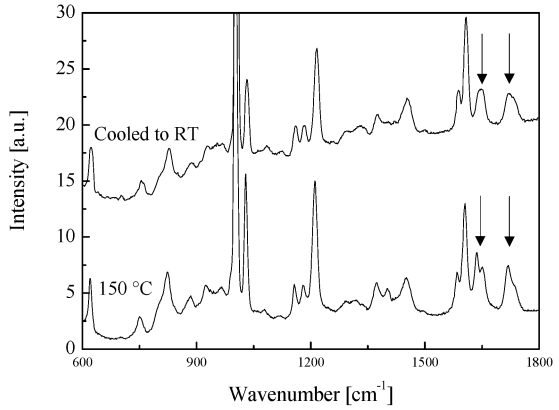

Figure 10. Raman spectra of the 60/40 wt % PBLG/BzMA sample at 150 °C and after cooling to room temperature. Arrows point to differences in the two spectra.

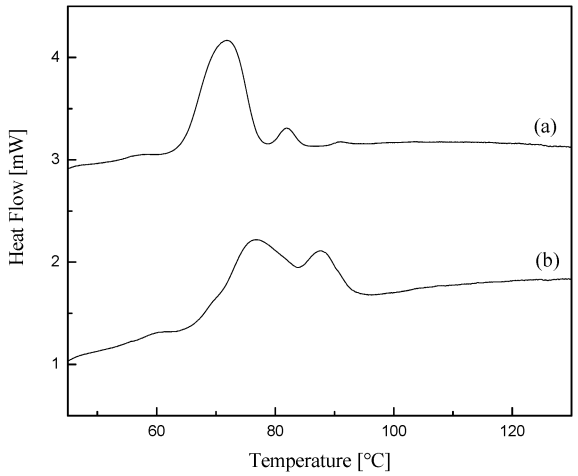

Figure 11. DSC traces upon heating of the PBLG/BzMA sample: (a) 30/70 wt %, (b) 60/40 wt %.

resulting in broadening of the peaks. Also for the WAXS data the reflections become less distinct upon cooling (Figure 8). The observed changes in both the Raman spectra and the diffraction pattern are attributed to a disordering process that occurs upon cooling the homogeneous samples. Hence, the presence of intercalated solvent within the hexagonal packing of the PBLG molecules disturbs both the helical conformation and the packing of the helices upon cooling.

3.2.4. Heat Effects Involved in Heating of Cast Films. Differential scanning calorimetry experiments for samples with different PBLG concentrations were performed to check whether the observed changes upon heating cast films correspond to real thermodynamic processes. As an example, DSC traces of cast films of PBLG with BzMA containing 30 and 60 wt % PBLG, on heating, are presented in parts a and b, respectively, of Figures 11.

Upon heating the cast films, both samples show two endotherms. The temperature of the maximum of these endotherms increases with increasing polymer concentration. For the 30/70 wt % PBLG/BzMA sample the peak maxima are at 72 and 82 °C, whereas for the 60/40 wt % PBLG/BzMA sample the maxima are found at 77 and 88 °C. The enthalpy of the first endotherm is roughly the same for both samples (4.3 J•g^{-1}), while the enthalpy of the second endotherm increases with polymer concentration.

The mechanically flexible nature of the PBLG/BzMA films similar to that of gels obtained from semicrystalline polymers (for example, partially dried high molar mass polyethylene in xylene/decalin) suggests that also for the PBLG/BzMA system a gel is formed. In the literature, two different kinds of explanations are given to the occurrence of two endotherms upon heating PBLG gels. The two endotherms occur either due to the presence of two different types of clusters[13,16,26] or due to a two-stage melting process of one type of clusters.[18,19]

The explanation of two endotherms by a two-step melting process does not seem to be in agreement with the WAXS results. The associated partial breaking of clusters into elementary fibrils should result in a shift in the small-angle region of the diffraction pattern. However, heating results in a disappearance of the high intensity close to the beamstop without any shift in d value and for samples with a high polymer concentration in an additional disappearance of the reflection at $d = 34$ Å.

The explanation of the two endotherms by the presence of two types of clusters (complex phase and pure PBLG phase)[16] seems to be consistent with the WAXS results. According to this idea, the cast film consists of polymer-rich domains (in which clusters of both the complex phase and pure PBLG are present) and solvent-rich domains. The first endotherm in the DSC trace is observed at a temperature similar to that of the decrease of the high intensity close to the beamstop in the WAXS pattern. This suggests attributing the endotherm to melting of the complex phase in the polymer-rich domains. Due to the melting of the complex phase, the polymer-rich and solvent-rich phases partially homogenize and the reflection arising from the average distance between these domains vanishes. The second endotherm in the DSC trace can be attributed to dissolution of bundles of rigid rods of PBLG. Since a higher polymer concentration can be expected to result in larger bundles, the enthalpy of the second endotherm will increase with increasing polymer concentration, as observed. The melting of the rigid rods, which results in homogenization of the sample, could be reflected in the WAXS pattern by the disappearance of the second reflection. A small discrepancy in temperature is found between the two techniques for samples with a relatively high polymer concentration. For the 60/40 wt % PBLG/BzMA sample the maxima in the DSC trace are observed at slightly lower temperatures than the changes in the WAXS pattern. However, taking into account that the effects in the diffraction pattern are observed at a relatively late stage of the transition (i.e., at the end of the endotherm in DSC) and that the DSC endotherm is broad, the two characterization techniques are still in relatively good agreement. From the DSC trace of a sample with a relatively low polymer concentration, it is clear that the presence of clusters of pure PBLG will decrease with increasing solvent amount. The heat effect is so small that it can be quite well imagined that the number of clusters is so low that the process is not depicted by WAXS.

The results upon heating cast films of PBLG/BzMA can be summarized as follows: Upon heating the sample, first melting of the complex phase occurs in polymer-rich domains, followed by complete homogenization through dissolution of bundles of rigid rods. After homogenization, a hexagonal phase is obtained. The diffraction data show that this phase perfects upon heating. Cooling of the homogeneous samples results a disordering process of the complex phase. The splitting in the WAXS pattern of the inner reflection into two reflections corresponds to the complex phase and the pure PBLG phase.

3.3. Polymerization of the Solvent. As discussed in the previous section, upon heating PBLG/BzMA samples above 100 °C, homogenization occurs, ultimately resulting in intercalation of solvent molecules within the hexagonal packing of the

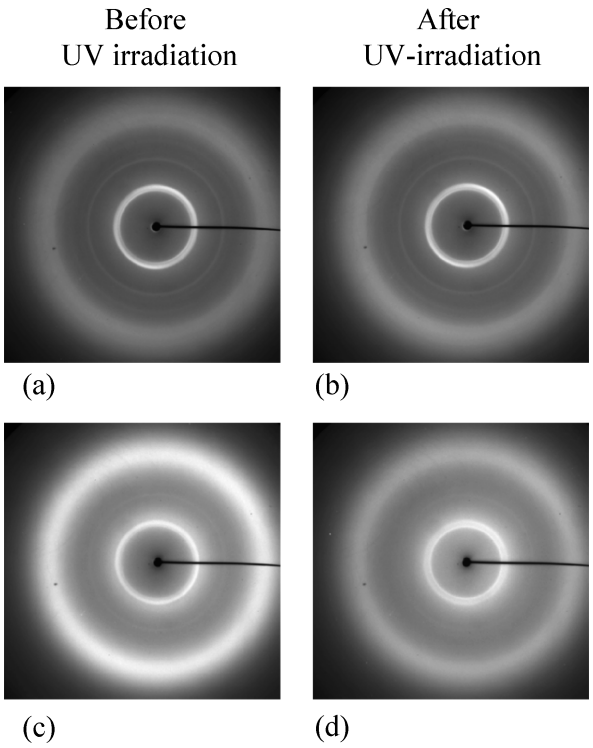

Figure 12. WAXS patterns upon polymerization of homogeneous PBLG/BzMA samples. (a) and (b) correspond to 35/65 wt % and (c) and (d) to 20/80 wt %.

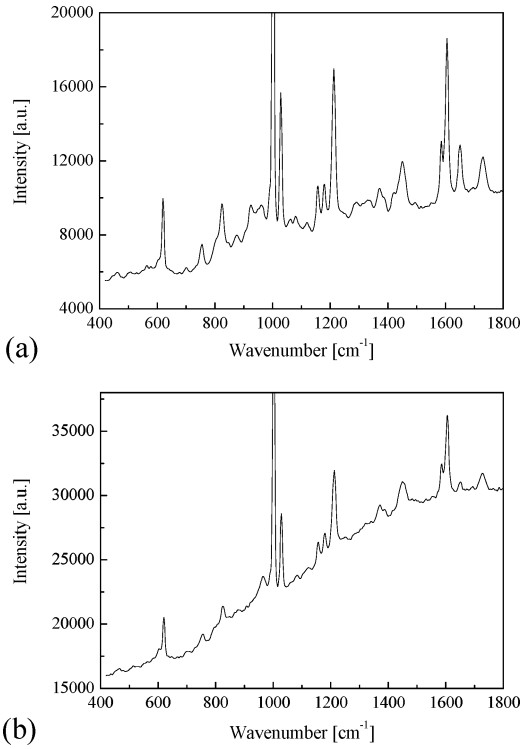

Figure 13. Raman spectra of polymerized homogeneous PBLG/BzMA samples: (a) 35/65 wt %, (b) 20/80 wt %.

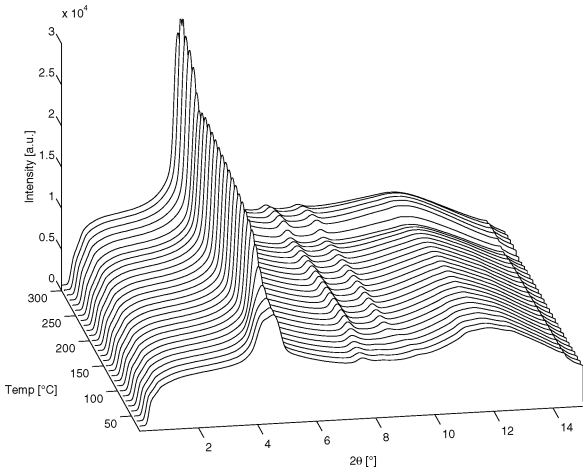

Figure 14. 3-D representation of WAXS patterns obtained upon heating a polymerized homogeneous 35/65 wt % PBLG/BzMA sample.

polymer chains. If the solvent stays intercalated upon polymerization, this could lead to a molecular blend of the polymer and the polymerized solvent. The polymerization of BzMA has been performed for samples heated to 150 °C to obtain a homogeneous system.[27] The WAXS data upon polymerization of the homogeneous samples (by means of UV irradiation at room temperature) are depicted in Figure 12. For the 35 wt % sample, where splitting of the inner reflection already occurred upon cooling, UV irradiation is only characterized by the incoming of a very weak halo just outside this inner reflection. UV irradiation of the 20/80 wt % PBLG/BzMA sample results in splitting of the inner reflection, while the relatively broad reflection which was present after cooling is maintained. From the minor changes which occur in the WAXS pattern after UV irradiation it is very difficult to conclude whether polymerization really takes place. To verify, Raman spectra of the UV-irradiated samples have been recorded.

The Raman spectrum of the UV-irradiated 35/65 wt % PBLG/BzMA sample is depicted in Figure 13a, while Figure 13b represents the Raman spectrum of the UV-irradiated 20/80 wt % PBLG/BzMA sample. Both spectra show the presence of a peak at 963 cm^{-1}, implying the presence of methacrylates. The absence of a peak at 1636 cm^{-1} (C═C stretching vibration) indicates that for both samples BzMA is polymerized upon UV irradiation.

From the WAXS data of the polymerized 20/80 wt % PBLG/BzMA sample it is clear that polymerization results in distortion of the hexagonal packing. After UV irradiation the inner reflection is split into two reflections at $2\theta = 4.1°$ ($d = 14.0$ Å) and 4.5° ($d = 12.7$ Å). The polymerization of pure BzMA is characterized by the incoming of a halo around $d = 11.8$ Å, which arises from the interchain distance of PBzMA. For the homogeneous samples, this halo is also present but the intensity is weak. A possible explanation for this difference can be that in the homogeneous sample a small correlation is present between the PBzMA molecules. Since most of the polymerized solvent will be present as separate chains between the PBLG molecules, much less correlation exists between the PBzMA molecules compared to pure PBzMA, and therefore, the polymerization is not reflected by the incoming of a relatively strong halo from the interchain distance.

To verify the stability of the polymerized samples, a heating experiment has been performed for the polymerized homogeneous samples and monitored in situ by wide-angle X-ray diffraction. Figure 14 represents the 3-D WAXS data upon heating a polymerized homogeneous sample. Upon heating, the splitting of the inner reflection disappears, while the reflections at higher angles become more pronounced. At 200 °C reflections are present at $2\theta = 4.3°$ ($d = 13.3$ Å), $2\theta = 7.4°$ ($d = 7.7$ Å), and $2\theta = 8.6°$ ($d = 6.7$ Å). Compared to those of the unpolymerized sample (Figure 7), the values are shifted to slightly smaller d values. Evidently, polymerization leads to a slight contraction of the unit cell. This proves once more that

solvent molecules are really present between the helices of PBLG, because in the case of separate domains of polymer and solvent polymerization of BzMA should have no influence on the packing of the crystalline phase.

From the polymerization experiments of the homogeneous samples, several conclusions can be drawn: The absence of a strong reflection of the interchain distance of PBzMA after UV irradiation of the homogeneous sample indicates that no correlation is present between the PBzMA molecules. Upon polymerization, the homogeneous sample slightly distorts, but upon heating, the hexagonal packing is recovered. Moreover, due to the polymerization some contraction occurs, resulting in slightly smaller *d* values of the (010)/(100) reflection compared to those of the unpolymerized samples. All these results suggest that solvent is indeed present between the PBLG helices, even after polymerization. This implies that for the PBLG/BzMA system a molecular blend of the polymer and the polymerized solvent is obtained.

4. Concluding Remarks

From the present results, the following conclusions can be drawn.

(1) In the cast films separate zones of PBLG and BzMA are present. Upon heating the films, homogenization takes place and the chains pack in a hexagonal phase, similar to those of pure PBLG. Since in the WAXS pattern no intensity is observed below $2\theta = 1°$, it can be concluded that the system is homogeneous at the molecular level. DSC experiments show that the observed changes upon heating the cast films are real thermodynamic processes.

(2) Due to intercalation of solvent molecules between the helices of PBLG, a regular ordering of the solvent molecules is obtained. This gives rise to a relatively broad reflection around 12.2 Å ($2\theta = 4.7°$). Upon cooling the homogeneous sample, disordering of the hexagonal packing occurs.

(3) Polymerization of the homogeneous samples results in a further disordering of the hexagonal packing. The *d* values shift to slightly lower values, indicating a contraction of the unit cell.

(4) The influence of polymerization on the *d* values and the absence of any intensity in the small-angle region of the WAXS pattern prove that after polymerization a molecular blend between PBLG and PBzMA is obtained. This is because if phase separation between the polymer and the solvent were to occur, polymerization would have no influence on the crystal packing and similar to the cast films some intensity would be observed in the small-angle region of the WAXS pattern.

The overall conclusion is that with the PBLG/BzMA system a homogeneous material can be obtained. Since polymerization does not result in phase separation, this method can be used to control the morphology of the two polymers on a molecular scale. It is to be noted that it has not been possible to blend PBLG and PBzMA directly at the molecular level.

References and Notes

(1) Bamford, C. H.; Elliott, A.; Hanby, W. E. *Synthetic Polypeptides*; Academic Press: New York, 1956.
(2) Elliott, A.; Ambrose, E. J. *Discuss. Faraday Soc*. **1950**, *9*, 246.
(3) Doty, P.; Bradbury, J. H.; Holtzer, A. M. *J. Am. Chem. Soc.* **1956**, *78*, 947.
(4) Robinson, C.; Ward, J. C. *Nature* **1957**, *30*, 1183.
(5) Parry, D. A. D.; Elliott, A. *J. Mol. Biol.* **1967**, *25*, 1.
(6) Squire, I. M.; Elliott, A. *Mol. Cryst. Liq. Cryst.* **1969**, *7*, 457.
(7) Russo, P. S.; Miller, W. G. *Macromolecules* **1983**, *16*, 1690.
(8) Uematsu, I.; Uematsu, Y. *Adv. Polym. Sci.* **1954**, *59*, 38.
(9) Horton, J. C.; Donald, A. M.; Hill, A. *Nature* **1990**, *346*, 44.
(10) Flory, P. J. *Proc. R. Soc. London, A* **1956**, *234*, 73.
(11) Wee, E. L.; Miller, W. G. *J. Phys. Chem.* **1971**, *75* (10), 1446.
(12) Miller, W. G.; Kou, L.; Tohyama, K.; Voltaggio, V. *J. Polym. Sci., Polym. Symp.* **1978**, *65*, 91.
(13) Sasaki, S.; Hikata, M.; Shiraki, C.; Uematsu, I. *Polym. J.* **1982**, *14*, 205.
(14) Sasaki, S.; Tokuma, K.; Uematsu, I. *Polym. Bull.* **1983**, *10*, 539.
(15) Ginzburg, B.; Siromyatnikova, T.; Frenkel, S. *Polym. Bull.* **1985**, *13*, 139.
(16) Hill, A.; Donald, A. M. *Polymer* **1988**, *29*, 1426.
(17) Horton, J. C.; Donald, A. M. *Polymer* **1991**, *32*, 2418.
(18) Prystupa, D. A.; Donald, A. M. *Macromolecules* **1993**, *26*, 1947.
(19) Cohen, Y.; Dagan, A. *Macromolecules* **1995**, *28*, 7638.
(20) van Hooy-Corstjens, C. S. J. Ph.D. Thesis, Eindhoven University of Technology, 2002.
(21) Koenig, J. L. *J. Polym. Sci., Part D: Macromol. Rev.* **1972**, 59.
(22) Koenig, J. L.; Sutton, P. L. *Biopolymers* **1971**, *10*, 89.
(23) Watanabe, J.; Kazamichi, I.; Gehani, R.; Uematsu, I. *J. Polym. Sci., Polym. Phys. Ed.* **1981**, *19* (4), 653.
(24) McKinnon, A. J.; Tobolsky, A. V. *J. Phys. Chem.* **1968**, *72*, 1157.
(25) Corstjens, C. S. J.; Rastogi, S.; Lemstra, P. J. *Macromol. Symp.* **1999**, *138*, 105.
(26) Izumi, Y.; Takezawa, H.; Kikuta, N.; Uemura, S.; Tsutsumi, A. *Macromolecules* **1998**, *31*, 430.
(27) Corstjens, C. S. J.; Rastogi, S.; Lemstra, P. J. *Macromol. Symp.* **1999**, *138*, 111.

BM050817Q